Bioorganic Chemistry 86 (2019) 393–400

Contents lists available at ScienceDirect

Bioorganic Chemistry

journal homepage: www.elsevier.com/locate/bioorg

Anti-inflammatory drug approach: Synthesis and biological evaluation of novel pyrazolo[3,4-*d*]pyrimidine compounds

Noor Atatreh[a], Amal M. Youssef[a,b,*], Mohammad A. Ghattas[a], Mohammad Al Sorkhy[a], Sara Alrawashdeh[a], Khaled B. Al-Harbi[c], Ibrahim M. El-Ashmawy[c,d], Tariq I. Almundarij[c], Amani A. Abdelghani[e], Alaa S. Abd-El-Aziz[e]

[a] College of Pharmacy, Al Ain University of Science and Technology, Al Ain, United Arab Emirates
[b] Department of Pharmaceutical Chemistry, Faculty of Pharmacy, Alexandria University, Alexandria, Egypt
[c] Department of Veterinary Medicine, College of Agricultural and Veterinary Medicine, Qassim University, Saudi Arabia
[d] Department of Pharmacology, Faculty of Veterinary Medicine, Alexandria University, Alexandria, Egypt
[e] Department of Chemistry, University of Prince Edward Island, Charlottetown, Prince Edward Island C1A 4P3, Canada

ARTICLE INFO

Keywords:
Synthesis
Pyrazolo[3,4-*d*]pyrimidines
Anti-inflammatory drugs
Docking
COX inhibitor

ABSTRACT

In this study, the acid chlorides of pyrazolo[3,4-*d*]pyrimidine compounds were prepared and reacted with a number of nucleophiles. The novel compounds were experimentally tested via enzyme assay and they showed cyclooxygenase-2 inhibition activity in the middle micro molar range (**4b** had a COX-1 IC_{50} of 26 μM and a COX-2 IC_{50} of 34 μM, **3b** had a COX-1 IC_{50} of 19 μM and a COX-2 IC_{50} of 31 μM, **3a** had a COX-2 IC_{50} of 42 μM). These compounds were analyzed via docking and were predicted to interact with some of the COX-2 key residues. Our best hit, **4d** (COX-1 IC_{50} of 28 μM, COX-2 IC_{50} of 23 μM), appears to adopt similar binding modes to the standard COX-2 inhibitor, celecoxib, proposing room for possible selectivity. Additionally, the resultant novel compounds were tested in several *in vivo* assays. Four compounds **3a** (COX-2 IC_{50} of 42 μM), **3d**, **4d** and **4f** were notable for their anti-inflammatory activity that was comparable to that of the clinically available COX-2 inhibitor celecoxib. Interestingly, they showed greater potency than the famous non-steroidal anti-inflammatory drug, Diclofenac sodium. In summary, these novel pyrazolo[3,4-*d*]pyrimidine analogues showed interesting anti-inflammatory activity and could act as a starting point for future drugs.

1. Introduction

Pyrazolopyrimidines are fused heterocyclic compounds that have considerable chemical and pharmacological importance as purine analogs. They are of interest as potential bioactive molecules. They exhibit wide pharmacological activities like tuberculostatic [1] antimicrobial [2], neuroleptic [3], antitumor [1], antihypertensive [4] and anti-leishmanial activities [5]. They may act as tropomyosin receptor kinase (Trk) and c-Src inhibitors [6,7], C−C chemokine receptor type 1 and purine antagonists [8], HIV reverse transcriptase inhibitors [9] as well as showing activity as antitumor/anti-leukemia [10–13] and herbicidal/fungicidal agents [14].

Several compounds as xanthene attached amino acids [15], piperazine-1-carbothioamide chitosan silver nanoparticles [16], dihydrazones [17], coumarins [18], benzo[*d*]thiazoles [19] and sulfur containing motifs [20] have exhibited anti-inflammatory activities. The anti-inflammatory properties of pyrazolo[3,4-*d*]pyrimidine compounds as potential inhibitors of cyclooxygenase (COX) [21] and p38α isoenzymes [22,23] are well known and gaining more interest. Traditional non-steroidal anti-inflammatory drugs (NSAIDs) are still the most commonly prescribed medications to alleviate acute and chronic inflammation, pain and fever. The mechanism of action of NSAIDs is lowering the production of inflammatory mediators such as prostaglandins (PGs). They inhibit the cyclooxygenase enzyme (COX) that catalyzes the biosynthesis of prostaglandins (PGs) and thromboxanes from arachidonic acid [24].

There are two COX isoforms COX-1 and COX-2 [25]. COX-1 is the constitutive isoform which is mainly responsible for the synthesis of cytoprotective PGs in gastrointestinal (GI) tract, maintenance of renal function in the kidney [26]. The inducible isoform COX-2 plays a major role in PG biosynthesis in inflammatory cells [27]. It is believed that inhibition of COX-1 results in GI damage, ulceration, hematologic effects and nephrotoxicity [28]. Therefore, highly selective COX-2 inhibitors (or “coxibs”) have been developed to alleviate pain and

* Corresponding author at: College of Pharmacy, Al Ain University of Science and Technology, P.O. Box: 64141, Al Ain, United Arab Emirates.
E-mail address: ayoussef65@yahoo.com (A.M. Youssef).

https://doi.org/10.1016/j.bioorg.2019.02.014
Received 17 December 2018; Received in revised form 3 February 2019; Accepted 4 February 2019
Available online 05 February 2019
0045-2068/

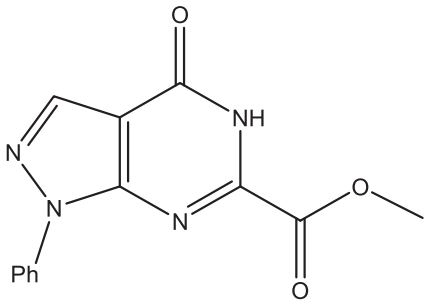

Fig. 1. Structure of compound **1**.

inflammation without the untoward side effects associated with non-selective NSAIDs. Among this class of compounds is celecoxib; 4-[5-p-tolyl-3-(trifluoromethyl)-1*H*-pyrazol-1-yl]benzenesulfonamide, which is a pyrazole derivative that is known to inhibit COX-2 selectively [29]. However, its long-term use is associated with cardiovascular adverse effects [30]. Therefore, there is a need for the development of novel drugs having anti-inflammatory activity with better safety profile.

Methyl 4,5-dihydro-4-oxo-1-phenyl-1H-pyrazolo[3,4-*d*]pyrimidine-6-carboxylate **1** [31] (Fig. 1) which was previously prepared in our lab, was found to be toxic to monocytes at 40 μM and also showed a neuroprotective effect at 20 μM (2-fold difference). This compound showed *in vitro* anti-neurotoxic and neuroprotective activity at concentrations below its toxic range and partially inhibited both COX-1 and COX-2 enzymes.

As a continuation of our research program on the synthesis of novel anti-inflammatory agents, the objectives of the present investigation have been directed toward the synthesis of new derivatives of pyrazolo [3,4-*d*]pyrimidines. The new derivatives incorporate various linear and branched chains in addition to morpholino group and aromatic moieties. The different derivatives attached to pyrazolopyrmidine ring at position-2 have been synthesized in order to investigate their impact on the anticipated anti-inflammatory activity.

The new compounds were investigated *in vitro* and *in vivo* for their anti-inflammatory activity. Docking was conducted for these compounds to suggest their binding mode and correlate that with biological activities.

2. Results and discussion

2.1. Chemistry

Synthetic strategies adopted for the synthesis of the intermediate and target compounds are depicted in Scheme 1.The general intermediate, 5-amino-4-cyano-1-phenylpyrazole **2**was obtained through the reaction of phenyl hydrazine with commercially available ethoxymethylenemalononitrile in alcohol with a good yield [32].

Reaction of **2** with oxalyl chloride produced the acid chloride of pyrazolo[3,4-*d*]pyrimidine which was immediately reacted with different nucleophiles such as alcohols and amines to produce **3a-d** and **4a-f**, respectively.

The synthesized compounds were supported by spectroscopic data. IR spectra of **3a-d** and **4a-f** lacked CN absorption bands and showed vibrational bands at 1735–1739 cm^{-1}(CO ester) and 1686–1695 cm^{-1} (CO amide) which support the conversion of pyrazole-4-carbonitrile to the corresponding pyrazolo[3,4-*d*]pyrimidine esters and amides, respectively.

^{1}H NMR spectra of **3a-d** were characterized by the presence of a D_2O exchangeable singlet for the NH of pyrazolopyrmidine ring, a singlet for pyrazole-C_5-H, in addition to isopropyl, propyl, butyl and sec-butyl protons at the expected range of δ–ppm scale. DEPT 135 (Distortionless Enhancement of Polarization Transfer using a 135° decoupler pulse) of **3a** showed a carbon spectrum with methyl (CH_3) and methyne (CH) carbons appearing at 21.8 and 71.8 respectively, whereas DEPT 135 of **3b–d** showed methene (CH_2) carbon, in addition to the methyl (CH_3) and methyne (CH) carbons.

^{1}H NMR spectra of **4a-f** displayed the characteristic chemical signals corresponding to the pyrazolopyrmidine ring in addition to other protons which were observed at their expected chemical shifts, whereas DEPT 135 showed methyl (CH_3), methyne (CH) ormethene (CH_2) carbons for each compound at the expected range.

2.2. In vitro cyclooxygenase inhibition assay

The ability of our compounds to inhibit the conversion of Arachidonic acid (AA) to Prostaglandin H2 (PGH2) by human recombinant COX-1 and COX-2 was determined using a COX inhibitor screening assay kit Celecoxib served as positive control for COX-2 and Diclofenac for COX-1. The results show significant COX-2 inhibition for compounds **3b**, **4b** and **4d** as shown in Table 1. Remarkably, **4d** exhibited comparable inhibition percentage to that of Celecoxib, with an IC_{50} of 23.8 μM. On the other hand, compound **3b** showed more specificity toward COX-1when compared to Diclofenac with an IC_{50} of 19.45 μM and 86% inhibition, putting it in close proximity with the classical COX-1 inhibitor.

2.3. In vivo assays

The anti-inflammatory activity of ten compounds was evaluated by two screening protocols, namely the carrageenan-induced paw edema and turpentine oil–induced granuloma pouch bioassays. The paw edema was employed as a model for acute and sub-acute inflammation, while the turpentine oil–induced granuloma pouch assay was used as another model for sub-acute inflammation. The ED_{50} values of the most potent compounds were also determined. Both Diclofenac sodium and celecoxib (10 mg/kg) were used as reference drugs. The data obtained were presented in Tables 2–4 and expressed as means ± SE. Statistical differences of control and tested groups were carried out using the Analysis of Variance (ANOVA) followed by 'Student–Newman–Keuls Multiple Comparison Test'. They were performed using the Statistical Analysis System (SAS, 1987) computer package, SAS Incorporation Institute. The difference inresults was considered significant when $p < 0.05$.

2.3.1. Carrageenan-induced paw edema bioassay (Acute Inflammatory Model)

In this acute inflammatory model each test compound was dosed orally (po) at 10 mg/kg body weight 1 h prior to induction of inflammation by carrageenan injection. Celecoxib and dicofenac sodium were utilized as reference anti-inflammatory drugs at a dose of 10 mg/kg, po. The anti-inflammatory activity was then calculated at 1, 2, 3, and 4 hafter induction. The data obtained are presented in (Table 2) as the mean paw volume (mL) in addition to the percentage anti-inflammatory activity (AI %). All of the test compounds significantly reduced paw edema volume 1, 2, 3, and 4 h after induction. However, a comparison of the anti-inflammatory activity of the test compounds, relative to the control, indicated distinctive pharmacokinetic profiles.

A comparative study of the AI activity of tested compounds relative to the reference drugs at different time intervals indicated the following: after 1 h, compounds **3a**, **4c**, **4d** and **4f** showed distinctive pharmacokinetic profile as revealed from its potent AI activity (53%, 66%, 64% and 55%, respectively) and rapid onset of action which was higher than Diclofenac Na (51%). After 2 h interval, compounds **3a**, **4b**, **4d** and **4f** displayed significant inhibition of paw edema (55%, 55%, 65% and 63%, respectively) equipotent and higher than Diclofenac sodium(53%).Taking the AI activity after 4 h as acriterion for comparison, the data indicated that compounds **3a**, **3d**, **4b**, **4d** and **4f** displayed higher or equipotent inhibition of pawedema with percentage activity of 57–66% when compared with that of Diclofenac sodium

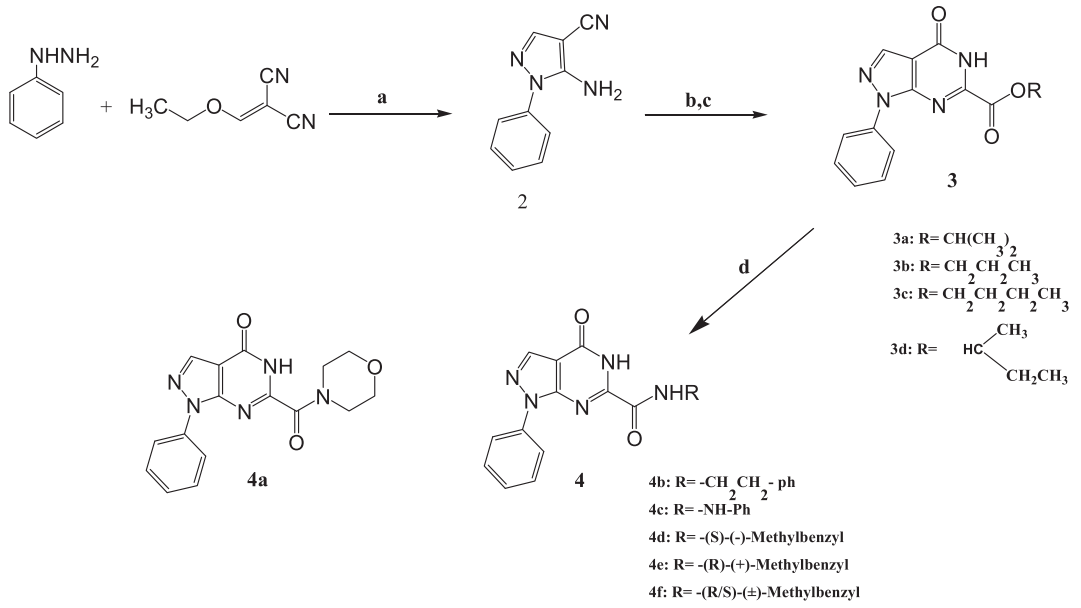

Scheme 1. Reagents and reaction conditions: (a) ethanol, rt, overnight; (b) COCl2, THF, rt, overnight; (c) ROH; (d) H2N-R, THF, reflux, 10-12hr.

Table 1
Data obtained from enzyme assay and expressed as means ± SE.

Comp. No.	% inhibition (40 μM)		IC_{50})μM(	
	COX-1	COX-2	COX-1	COX-2
3a	37.21	54.15	–	42.1 ± 0.29
3b	86.03	79.61	19.45 ± 0.07	31.4 ± 0.12
3c	78.17	47.76	–	–
3d	63.06	37.63	–	–
4a	13.50	19.65	–	–
4b	81.45	67.69	26.04 ± 0.36	34.4 ± 0.10
4c	26.04	14.91	–	–
4d	73.36	91.25	28.39 ± 0.03	23.8 ± 0.17
4e	19.07	23.50	–	–
4f	18.66	41.60	–	–
Celecoxib	–	96.61	–	11.7 ± 0.23
Diclofenac	94.83	–	8.72 ± 0.28	–

(57%) but less than that of celecoxib (69%).

The most active compounds **(3a**, **3d**, **4d** and **4f)** were further tested at 5, 10, 20, 40 and 50 mg/kg body weight in order to determine their ED_{50}values. The results revealed that compounds **3a**, **3d**, **4d** and **4f** (ED_{50} = 8.3, 8.1, 7.6 and 7.4 mg/kg, respectively) were found to be nearly equipotent to celecoxib (ED_{50} = 7.2 mg/kg).

2.3.2. Carrageenan-induced paw edema bioassay (sub-acute inflammatory model)

In this sub-acute inflammatory model, inflammation was induced by carrageenan injection on the first and third days, and test compounds were administered orally (at 10 mg/kg daily) for 7 days. Again, celecoxib and Diclofenac sodium were used as a reference anti-inflammatory agents in this assay. The anti-inflammatory activity was calculated at the 1st and 8th day after induction and the data presented in Table 3 as the mean paw volume and the percentage anti-

Table 2
Anti-inflammatory activity of compounds in the carrageenan-induced rat paw edema model (acute inflammatory model).

Treatment	Volume of edema				ED_{50}
	0	1 h	2 h	4 h	
Control	1.03 ± 0.01[a]	2.30 ± 0,02	2.90 ± 0.03	3.75 ± 0.02	
3a	1.06 ± 0.02	1.65 ± 0,01* (53)[b]	1.90 ± 0.01* (55)	2.10 ± 0.02* (61)	8.3
3b	0.90 ± 0.01	1.66 ± 0,01* (40)	1.80 ± 0.01* (51)	2.11 ± 0.03* (55)	
3c	1.05 ± 0.02	1.89 ± 0,02* (33)	1.95 ± 0.01* (51)	2.32 ± 0.02* (53)	
3d	0.98 ± 0.01	1.68 ± 0,01* (44)	1.88 ± 0.02* (51)	2.03 ± 0.02* (61)	8.1
4a	1.05 ± 0.01	2.01 ± 0,01* (24)	2.37 ± 0.01* (29)	2.70 ± 0.02* (39)	
4b	1.06 ± 0.01	1.85 ± 0,01* (37)	1.90 ± 0.02* (55)	2.21 ± 0.02* (57)	
4c	1.07 ± 0.02	1.50 ± 0,01* (66)	2.13 ± 0.02* (43)	2.36 ± 0.01* (52)	
4d	1.05 ± 0.01	1.50 ± 0,01* (64)	1.69 ± 0.01* (65)	2.01 ± 0.01* (64)	7.6
4e	1.08 ± 0.01	1.85 ± 0,01* (39)	2.17 ± 0.01* (41)	2.61 ± 0.02* (43)	
4f	1.16 ± 0.01	1.73 ± 0,02* (55)	1.85 ± 0.01* (63)	2.08 ± 0.01* (66)	7.4
Celecoxib	1.21 ± 0.02	1.56 ± 0,01* (72)	1.79 ± 0.02* (68)	2.03 ± 0.01* (69)	7.2
Declofenac Na.	1.06 ± 0.01	1.68 ± 0,01* (51)	1.93 ± 0.01* (53)	2.21 ± 0.01* (57)	

Number of animals = 5.
All compounds and drugs are given at the dose of 10 mg/kg orally.
* Significantly different compared to corresponding control $p \leq 0.05$.
[a] Values are expressed as Mean ± SEM.
[b] Values in parentheses are percent anti-inflammatory activity.

Table 3
Anti-inflammatory activity of compounds in the carrageenan-induced rat paw edema model (sub-acute inflammatory model).

Treatment	Volume of edema		
	0	1st day	8th day
Control	1.03 ± 0.01[a]	3.75 ± 0.02	4.06 ± 0.03
3a	1.06 ± 0.02	2.10 ± 0.02* (61)[b]	2.38 ± 0.02* (56)
3b	0.90 ± 0.01	2.11 ± 0.03* (55)	2.55 ± 0.02* (45)
3c	1.05 ± 0.02	2.32 ± 0.02* (53)	2.74 ± 0.03* (44)
3d	0.98 ± 0.01	2.03 ± 0.02* (61)	2.31 ± 0.02* (56)
4a	1.05 ± 0.01	2.70 ± 0.02* (39)	2.68 ± 0.01* (46)
4b	1.06 ± 0.01	2.21 ± 0.02* (57)	2.73 ± 0.02* (44)
4c	1.07 ± 0.02	2.36 ± 0.01* (52)	2.45 ± 0.01* (54)
4d	1.05 ± 0.01	2.01 ± 0.01* (64)	2.26 ± 0.01* (60)
4e	1.08 ± 0.01	2.61 ± 0.02* (43)	2.88 ± 0.02* (40)
4f	1.16 ± 0.01	2.08 ± 0.01* (66)	2.16 ± 0.02* (66)
Celecoxib	1.21 ± 0.02	2.03 ± 0.01* (69)	2.25 ± 0.01* (65)
Declofenac Na.	1.06 ± 0.01	2.21 ± 0.01* (57)	2.36 ± 0.01* (57)

Number of animals = 5.
All compounds and drugs aregiven at the dose of 10 mg/kg orally.
* Significantly different compared to corresponding control $p \leq 0.05$.
[a] Values are expressed as Mean ± SEM.
[b] Values in parentheses are percent of anti-inflammatory activity.

Table 4
Anti-inflammatory activity of compoundsin the turpentine oil–induced granuloma pouch model.

Treatment	Volume of exudates	% of inhibition
Control	2.24 ± 0.02[a]	–
3a	1.02 ± 0.01*	54
3b	1.42 ± 0.02*	36
3c	1.39 ± 0.02*	37
3d	1.08 ± 0.01*	51
4a	1.63 ± 0.02*	27
4b	1.49 ± 0.02*	33
4c	1.03 ± 0.01*	54
4d	1.09 ± 0.01*	51
4e	1.66 ± 0.01*	25
4f	1.03 ± 0.01*	54
Celecoxib	1.02 ± 0.01*	54
Declofenac Na.	1.09 ± 0.01*	51

Number of animals = 5.
All compounds and drugs are given at the dose of 10 mg/kg orally.
* Significantly different compared to control $p \leq 0.05$.
[a] Values are expressed as Mean ± SEM.

inflammatory activity relative to a control.

The obtained data revealed that, according to the measurements performed on both the 1st and 8th day, all tested compounds displayed significant anti-inflammatory activity. At day 1, compounds **3a**, **3d**, **4d** and **4f** showed significant AI activities (61–66%) when compared to Diclofenac Na (57%); while compounds **3b**, and **4b**showed AI activities (55% and 57%) similar to Diclofenac sodium. At day 8, compound **4f** demonstrated distinctive AI activity (66%) higher than Diclofenac sodium (57%) and similar to celecoxib (65%);whereas, compounds **3a, 3d**and **4d** showed an inhibition of paw edema (56–60%) higher than that of Diclofenac sodium (57%).

2.3.3. Turpentine oil-induced granuloma pouch bioassay

In this sub-acute inflammatory model, each test compound was administered orally (10 mg/kg) 1 h prior to turpentine oil injection and administration was continued for 7 days. At the 8th day, the volume of exudates (mL) was measured and the percentage of granuloma inhibition was calculated. Celecoxib and Diclofenac sodium were used as a reference drugs. Table 4 illustrates that all of the studied compounds significantly reduced the exudate volume when comparedto the control group of animals. Compounds **3a**, **4c**and **4f** appeared to be equipotent to celecoxib (54%) and higher than Diclofenac sodium (51%); whereas Compounds **3d** and **4d** showed similar AI to Diclofenac sodium. The *in vivo* experiments (Tables 1–3) demonstrated anti-inflammatory activity of compounds **3a**, **3d**, **4d** and **4f** in carrageenan paw edema model of acute inflammation, as well as in the carrageenan paw edema and turpentine oil-induced granuloma pouch assays (sub-acute inflammatory models). Therefore, these compounds might be effective in managing acute inflammation, as well as in controlling chronic inflammatory conditions.

2.4. Docking study

There are two main NSAIDs binding regions in the COX catalytic pocket: the top of the active site comprising Ser530 and Tyr385 (e.g. involved in Diclofenac binding) or the bottom of the active site comprising Arg120 and Tyr355 (e.g. involved in flurbiprofen binding) [33]. The above interactions are mainly electrostatics and are primarily formed by the NSAIDs' carboxylate. There is an additional binding region only accessed by selective COX-2 inhibitors containing four main residues Gln192, Ser353, Arg 513 and Val523.

In the present study, docking was employed to predict the binding modes of the tested compounds inside the target pocket. Table 5 shows the binding energies of our ten compounds docked into the COX-1 and COX-2 binding site. Docked compounds were predicted to have favorable binding energies although celecoxib showed a superior docking score compared to our hits. Interestingly, and in line with the *in vitro* and *in vivo* findings, **4d** was predicted to have the best docking score amongst all tested compounds against the COX-2 enzyme.

4d was predicted to have a docking score of −9.501 kcal/mol for COX-2 and 6.2 kcal/mol for COX-1, which comes consistent to the enzymatic assays results where **4d** possessed slighter greater selectivity to

Table 5
Docking results of test compounds into the COX-I and COX-II binding site.

Compound code	COX-2		COX-1		Lipinski's druglikeness	logP(o/w)	molecular weight
	Glide_XP Score (kcal/mol)	Ligand efficiency (kcal/mol)	Glide_XP Score (kcal/mol)	Ligand efficiency (kcal/mol)			
4d	−9.501	−0.351	−6.187	−0.229	1	2.20	359.38
4e	−9.334	−0.345	−5.182	−0.192	1	2.20	359.38
3c	−8.766	−0.380	−8.431	−0.367	1	1.99	312.32
4a	−8.641	−0.360	−7.513	−0.313	1	−0.28	325.32
4b	−8.638	−0.319	−8.039	−0.298	1	2.53	359.38
3d	−8.389	−0.364	−6.799	−0.296	1	2.01	312.38
3a	−8.243	−0.373	−6.705	−0.305	1	1.39	398.30
4c	−8.542	−0.314	−6.695	−0.257	1	1.50	346.34
3b	−8.139	−0.369	−6.744	−0.307	1	1.55	398.30
Celecoxib	−13.195	−0.507	–	–	1	3.11	381.37
Flurbiprofen	–	–	−13.804	−0.767	1	4.31	243.25

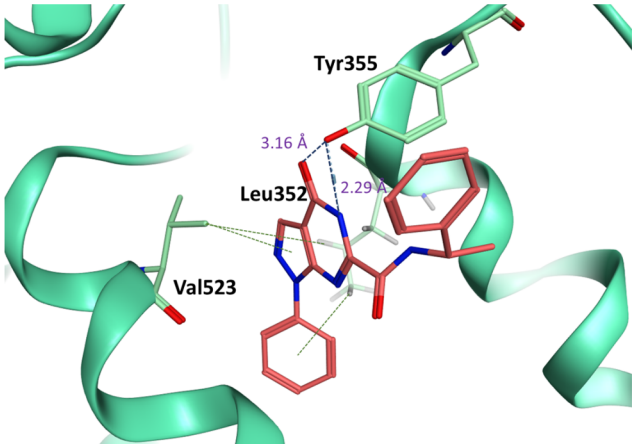

Fig. 2. The predicted binding mode of compound **4d** (pink sticks) inside the COX-2 binding site (green ribbon and sticks).

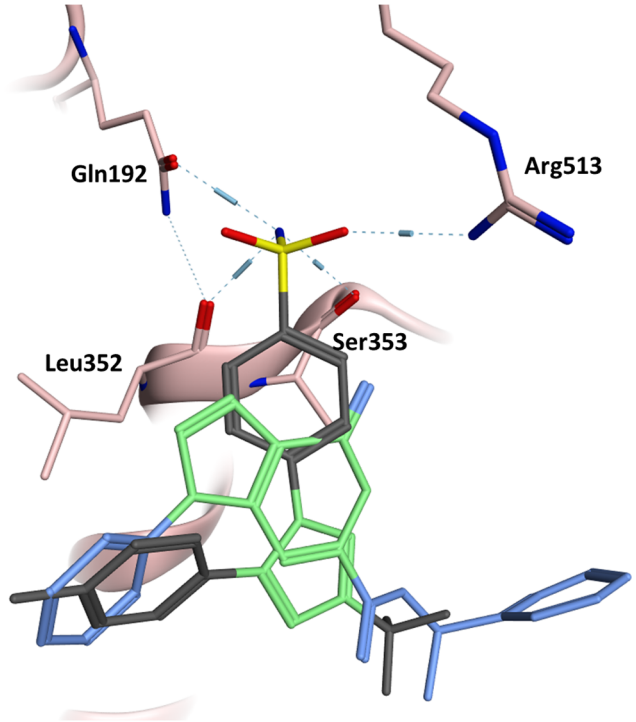

Fig. 3. The docked pose of **4d** superposed on the celecoxib co-crystallized structure inside the COX-2 binding site. The core ring systems are shown in green in all structures, **4d** is shown in blue, and celecoxib is shown in dark grey.

COX-2 than COX-1; though selectivity prediction was not consistent with experimental findings for other compounds. As shown in Figs. 2 and 4d forms hydrogen bonds with the key amino acid Tyr355 and several π-hydrogen interactions with the Leu352 and Val523 side chains along with multiple van der Waals contacts with the surrounding hydrophobic residues. Although **4d** does not possess a similar binding mode to celecoxib in the COX-2 active site, its pyrazolo[3,4-*d*]pyrimidine system seems to sit in the same site of celexocib's pyrazole ring, as shown in Fig. 3.

Although docking was able to predict the experimental superiority of **4d** over other tested analogues, it was not quite successful to explain why the other enantiomer **4e** showed weaker COX-2 inhibition *in vitro*. Instead, **4e** was predicted to have as low binding energy as **4d**; and looking at their docked poses aligned over each other showed that they have very similar binding mode apart from the methyl group orientation that appears sitting in opposite direction (Fig. 4).

When the *in vitro* activities and *in silico* findings are considered together, it can be suggested that:

(i) Our best hit **4d** was predicted to have its pyrazolo[3,4-*d*]pyrimidine scaffold sitting in the same place of celecoxib'spyrazole ring [33].
(ii) **4d** was also predicted to interact with the COX-2 key residues such as Tyr355 and Ser530.
(iii) **4d** showed promising experimental activity but only slight selectivity towards COX-2 which can be further enhance by optimizing the pyrazolopyrimidine ring binding so that it reaches the selectivity region in the COX-2 active site (Fig. 3).

3. Conclusion

Novel pyrazolo[3,4-*d*]pyrimidine compounds were prepared. Using enzymatic COX-1 and COX-2 inhibition assays the compounds were tested for their *in vitro* ability to inhibit COX-1 and COX-2. The results show significant COX-2 inhibition for compounds **3b**, **4b** and **4d**. The synthesized compounds were also evaluated for their *in vivo* anti-inflammatory activity using two different screening protocols, namely, carrageenan–induced paw edema and the turpentine oil-induced granuloma pouch bioassays. Among the tested analogs, compounds **3a**, **3d**, **4d** and **4f** were notable for their comparable anti-inflammatory effect to the clinically available COX-2 inhibitor celecoxib in both the acute inflammatory and sub-acute inflammatory models. The *in silico* findings come in line with the *in vivo* and *in vitro* assays results and also suggest that these compounds have the potential to be COX-2 selective inhibitors since they have typical binding modes of the benchmark drug celecoxib. Structure activity relationship showed that branched isomers **3a** and **3d** showed significant *in vitro* and *in vivo* COX-2inhibition. While linear isomer **3b** showed more specificity toward COX-1 inhibition. **4d** the enantiomer containing the bulky aromatic group was identified as the best compound adopting comparable activity to the clinically available COX-2 inhibitor celecoxib.

Based on all previously mentioned results,pyrazolo[3,4-d] pyrimidine-6-carboxylate and pyrazolo[3,4-*d*]pyrimidine-6-carboxamide derivatives could represent a fruitful matrix for the future development of a new class of anti-inflammatory agents.

4. Experimental

4.1. Chemistry

All chemicals and reagents were obtained from Sigma-Aldrich and were used without any further purification. All solvents were dried and stored over 3 Å molecular sieves before being used. Melting points were determined in open glass capillaries on a Stuart melting point apparatus and are uncorrected. The infrared (IR) spectra were recorded on a FTIR Nicolet IR 200 spectrophotometer. A Bruker Avance NMR spectrometer (^{1}H, 300 MHz and ^{13}C, 75 MHz) was used to characterize all synthesized complexes in DMSO-$d_6$with the chemical signals referenced to solvent residual signal in ppm. Elemental analyses for all the synthesized compounds were within ± 0.4% of the theoretical values. Follow-up of the reactions and checking the homogeneity of the compounds were made by TLC on silica gel-protected glass plates, and the spots were detected by exposure to UV-lamp at λ 254.

4.1.1. Subsbstituted-4-oxo-l-phenyl-4,5-dihydro-1H-pyrazolo[3,4-d] pyrimidine-6-carboxylate (3)

To a stirred solution of oxalyl chloride (l.27 g, 0.01 mol) in THF (5 mL), a solution of 5-amino-1 phenyl-1H-pyrazole-4-carbonitrile **2** (0.92 g, 0.005 mol) in THF (5 mL) was added dropwise over a period of 2 h. The reaction mixture was further stirred for 24 h atroom temperature (rt). The solvent was evaporated under reduced pressure, and the formed product was filtered, dried and refluxed in excess alcohol for

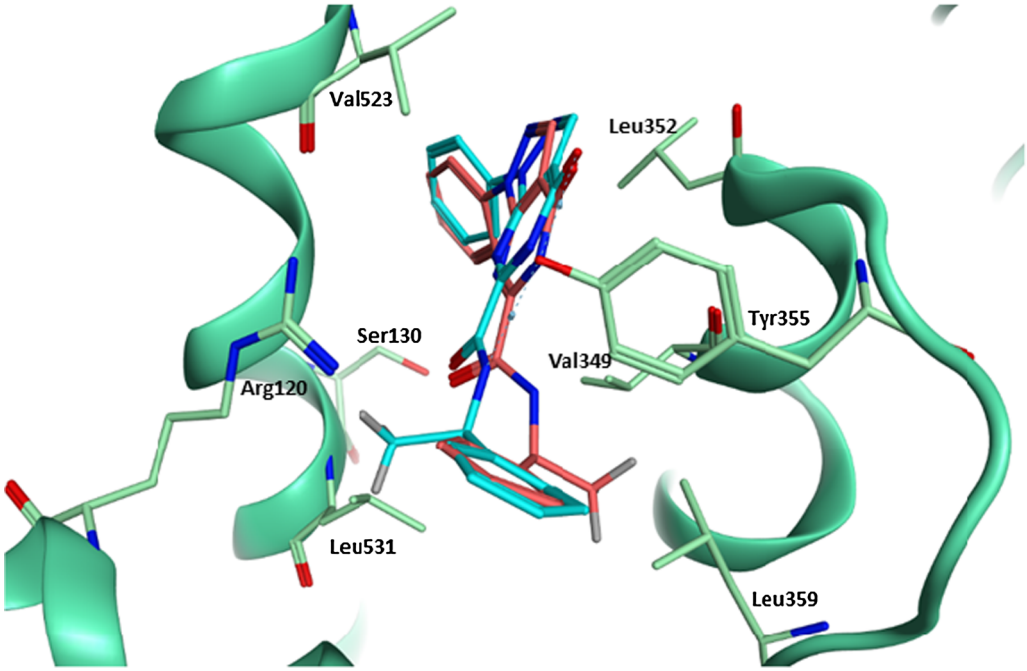

Fig. 4. The predicted binding mode of compound **4d** (pink sticks) and **4e** (cyan sticks) inside the COX-2 binding site (green ribbon and sticks).

5 min. The beige crystals were collected by suction filtration.

4.1.1.1. Isopropyl 4-oxo-1-phenyl-4,5-dihydro-1H-pyrazolo[3,4-d]pyrimidine-6-carboxylate (3a). Yield 85%; mp 158–160 °C.IR (cm^{-1}): 1738 (CO ester), 1686 (CO amide); ^{1}H NMR (δ ppm): 12.84 (s, 1H, NH, D_2O exchangeable), 8.42 (s, IH, pyrazole-C_5-H), 8.05–7.42 (m, 5H, aromatic-H), 4.1–3.8 (m, 1H, CH), 1.36 (d, J = 6.6 Hz, 6H, 2 CH_3,); ^{13}C NMR (δppm): 136.7, 129.8, 127.9, 122.4, 71.8, 21.8. Anal.Calcd for $C_{15}H_{14}N_4O_3$ (298.3): C, 60.40; H, 4.73; N, 18.78. Found: C, 60.75; H, 4.84; N, 18.39.

4.1.1.2. Propyl 4-oxo-1-phenyl-4,5-dihydro-1H-pyrazolo[3,4-d] pyrimidine-6-carboxylate (3b). Yield 80%; mp 164–166 °C. IR (cm^{-1}): 1735 (CO ester), 1692 (CO amide); ^{1}H NMR (δ ppm): 12.87 (s, 1H, NH, D_2O exchangeable), 8.43 (s, IH, pyrazole-C_5-H), 8.06–7.41 (m, 5H, aromatic-H), 4.3 (t, J = 13.2 Hz, 2H, CH_2), 1.80–1.69 (m, 2H, CH_2), 0.98 (t, J = 15.3 Hz,3H, CH_3); ^{13}C NMR (δ ppm): 136.7, 129.8, 127.9, 122.3, 68.6, 21.8, 10.6. Anal.Calcd for $C_{15}H_{14}N_4O_3$ (298.3): C, 60.40; H, 4.73; N, 18.78. Found: C, 60.05; H, 4.93; N, 19.15.

4.1.1.3. Butyl 4-oxo-1-phenyl-4,5-dihydro-1H-pyrazolo[3,4-d] pyrimidine-6-carboxylate (3c). Yield 82% ; mp 167–169 °C.IR (cm^{-1}): 1739 (CO ester), 1695 (CO amide); ^{1}H NMR (δ ppm): 12.91 (s, 1H, NH, D_2O exchangeable), 8.43 (s, IH, pyrazole-C_5-H), 8.07–7.41 (m, 5H, aromatic-H), 4.35 (t, J = 13.2 Hz, 2H, CH_2), 1.77–1.67 (m, 2H, CH_2), 1.50–1.38 (m, 2H, CH_2), 0.95 (t, J = 14.7 Hz, 3H, CH_3); ^{13}C NMR (δ ppm): 136.7, 129.8, 127.9, 122.3, 67.0, 30.3, 19.1, 14.2. Anal.Calcd for $C_{16}H_{16}N_4O_3$ (312.32): C, 61.53; H, 5.16; N, 17.94. Found: C, 61.85; H, 4.95; N, 18.30.

4.1.1.4. sec-Butyl 4-oxo-1-phenyl-4,5-dihydro-1H-pyrazolo[3,4-d] pyrimidine-6-carboxylate (3d). Yield 80%; mp 162–164 °C.IR (cm^{-1}): 1737 (CO ester), 1686 (CO amide); ^{1}H NMR (δppm): 12.89 (s, 1H, NH, D_2O exchangeable), 8.43 (s, IH, pyrazole-C_5-H), 8.08–7.41 (m, 5H, aromatic-H), 4.5–4.2 (m, IH, CH), 1.79–1.63 (m, 2H, CH_2), 1.32 (d, J = 6.3 Hz, 3H, CH_3), 0.94 (t, J = 15.9 Hz, 3H, CH_3); ^{13}C NMR (δ ppm): 136.7, 129.8, 127.9, 122.3, 76.1, 28.5, 19.4, 9.8. Anal.Calcd for $C_{16}H_{16}N_4O_3$ (312.32): C, 61.53; H, 5.16; N, 17.94. Found: C, 61.15; H, 5.34; N, 18.34.

4.1.2. Substituted 4-oxo-1-phenyl-4,5-dihydro-1H-pyrazolo[3,4-d]pyrimidine-6-carboxamide (4a-f)

A mixture of carboxylate derivative **3a**(0.3 g, 0.001 mol) and the appropriate amine (0.004 mol) in dry THF (10 mL) was heated under reflux for 10–12 h. The solvent was evaporated under reduced pressure, diethyl ether was added and the formed product was filtered, washed with diethyl ether, dried and crystallized from chloroform–hexane.

4.1.2.1. 6-(morpholine-4-carbonyl)-1-phenyl-1H-pyrazolo[3,4-d] pyrimidin-4(5H)one (4a). Yield 80%; mp 138–140 °C.IR (cm^{-1}): 1685, 1667 (CO amide); ^{1}H NMR (δ ppm): 12.21 (s, 1H,NH, D_2O exchangeable), 8.38 (s, 1H, pyrazole-C_5-H), 7.99–7.39 (m, 5H, aromatic-H), 3.68–3.53 (m, 8H, CH_2); ^{13}C NMR (δ ppm): 136.6, 129.8, 127.7, 122.3, 66.6, 47.1. Anal.Calcd for $C_{16}H_{15}N_5O_3$ (325.32): C, 59.07; H, 4.65; N, 21.53. Found: C, 59.37; H, 4.55; N, 21.88.

4.1.2.2. 4-oxo-N-phenethyl-1-phenyl-4,5-dihydro-1H-pyrazolo[3,4-d] pyrimidine-6-carboxamide(4b). Yield 85%; mp 170–172 °C.IR (cm^{-1}): 1686, 1664 (CO amide); ^{1}H NMR (δ ppm): 12.65 (s, 1H,NH, D_2O exchangeable), 8.45 (s, 1H, pyrazole-C_5-H), 8.22–7.52 (m, 10*H*, aromatic-H), 3.57–3.50 (m, 2H, CH_2), 2.89–2.83 (m, 2H, CH_2); ^{13}C NMR (δ ppm): 136.3, 129.6, 129.1, 128.9, 126.9, 126.7, 121.4, 41.2, 35.3. Anal. Calcd for $C_{20}H_{17}N_5O_2$ (359.38): C, 66.84; H, 4.77; N, 19.49. Found: C, 66.53; H, 4.57; N, 19.87.

4.1.2.3. 4-oxo-N',1-diphenyl-4,5-dihydro-1H-pyrazolo[3,4-d] pyrimidine-6-carbohydrazide (4c). Yield 78%; mp 177–179 °C.IR (cm^{-1}): 1692, 1664 (CO amide); ^{1}H NMR (δ ppm): 12.60 (s, 1H, NHD_2O exchangeable), 10.87 (s, IH, NH, D_2O exchangeable), 8.43 (s, IH, pyrazole-C_5-H), 8.29–6.74 (m, 10H, aromatic-H); ^{13}C NMR (δppm): 136.8, 129.8, 129.2, 127.6, 122.1, 119.5, 113.0. Anal.Calcd for $C_{18}H_{14}N_6O_2$ (346.34): C, 62.42; H, 4.07; N, 24.27. Found: C, 62.72; H, 4.25; N, 24.59.

4.1.2.4. S-(-)-4-oxo-1-phenyl-N-(1-phenylethyl)-4,5-dihydro-1H-pyrazolo [3,4-d] pyrimidine-6-carboxamide (4d). Yield 83%; mp 160–162 °C.IR (cm^{-1}): 1690, 1664 (CO amide); ^{1}H NMR (δ ppm): 12.37 (s, 1H, NH, D_2O exchangeable), 9.19 (s, IH, NH, D_2O exchangeable), 8.39 (s, IH, pyrazole-C_5-H), 8.19–7.24 (m, 10H, aromatic-H), 5.16 (q,

J = 7.2 Hz,1H, CH), 1.54 (d, J = 7.2 Hz, 3H, CH_3); ^{13}C NMR (δ ppm): 136.7, 129.8, 128.8, 127.7, 127.5, 126.6, 122.2, 49.4, 22.3. Anal.Calcd for $C_{20}H_{17}N_5O_2$ (359.38): C, 66.84; H, 4.77; N, 19.49. Found: C, 66.49; H, 4.58; N, 19.17.

4.1.2.5. R-(+)-4-oxo-1-phenyl-N-(1-phenylethyl)-4,5-dihydro-1H-pyrazolo[3,4-d]pyrimidine-6-carboxamide (4e). Yield 82%; mp 160–162 °C. IR (cm-^{1}): 1690, 1664 (CO amide); ^{1}H NMR (δ ppm): 12.37 (s, 1H, NH, D_2O exchangeable), 9.19 (s, IH, NH, D_2O exchangeable), 8.39 (s, IH, pyrazole-C_5-H), 8.19–7.24 (m, 10H, aromatic-H), 5.16 (q, J = 7.2 Hz,1H, CH), 1.54 (d, J = 7.2 Hz, 3H, CH_3); ^{13}C NMR (δ ppm): 136.7, 129.8, 128.8, 127.7, 127.5, 126.6, 122.2, 49.4, 22.3. Anal.Calcd for $C_{20}H_{17}N_5O_2$ (359.38): C, 66.84; H, 4.77; N, 19.49. Found: C, 67.18; H, 5.01; N, 19.85.

*4.1.2.6. **R/S-(±)-4-oxo-1-phenyl-N-(1-phenylethyl)-4,5-dihydro-1H-pyrazolo[3,4-d]pyrimidine-6-carboxamide (4f)***. Yield 85%; mp 160–162 °C.IR (cm^{-1}): 1690, 1664 (CO amide); ^{1}H NMR (δ ppm): 12.37 (s, 1H, NH, D_2O exchangeable), 9.19 (s, IH, NH, D_2O exchangeable), 8.39 (s, IH, pyrazole-C_5-H), 8.19–7.24 (m, 10H, aromatic-H), 5.16 (q, J = 7.2 Hz,1H, CH), 1.54 (d, J = 7.2 Hz, 3H, CH_3); ^{13}C NMR (δ ppm): 136.7, 129.8, 128.8, 127.7, 127.5, 126.6, 122.2, 49.4, 22.3. Anal.Calcd for $C_{20}H_{17}N_5O_2$ (359.38): C, 66.84; H, 4.77; N, 19.49. Found: C, 66.45; H, 4.55; N, 19.82.

4.2. In vitro cyclooxygenase inhibition assay

The inhibition of the conversion of AA toPGH2 by human recombinant COX-1 and COX-2 was determined using a COX inhibitor screening assay kit (No. 701230; Cayman Chemical, USA). The COX human inhibitor screening assay directly measures Prostaglandin F2alpha (PGF2α) by stannous chloride ($SnCl_2$) reduction of COX-derived PGH2 produced in the COX reaction. The prostanoid product is quantified via enzyme-linked immunosorbent assay (ELISA) using a broadly specific antiserum that binds to all the major PG compounds.

Cyclooxygenase inhibitory activity of **3a-d** and **4a-f** towards COX-1 and COX-2 activity was performed in accordance to the one recommended by the supplier of the kit. Celecoxib (Sigma, Germany) served as positive control for COX-2 and Diclofenac (Sigma, Germany) for COX-1. The test compounds were dissolved in DMSO for a final concentration in the reaction tubes of 40 μMin the screening run and 5 different concentrations which were 10, 20, 40, 80 and 100 μM in theIC_{50} run.

4.2.1. AChE competitive ELISA

This assay is based on the competition between PGs and a PG-acetylcholinesterase (AChE) conjugate (PG tracer) for a limited amount of PG antiserum. Because the concentration of the PG tracer is held constant while the concentration of PG varies, the amount of PG tracer that is able to bind to the PG antiserum will be inversely proportional to the concentration of PG in the well. This rabbit antiserum-PG (either free or tracer) complex binds to a mouse monoclonal anti-rabbit antibody that has been previously attached to the well. The plate is washed to remove any unbound reagents and then Ellman's Reagent (which contains the substrate to AChE) is added to the well. The yellow product of this enzymatic reaction is determined spectrophotometrically in a Microplate Reader (Multiskan™ GO Microplate Spectrophotometer) at 415 nm. The intensity of this color is proportional to the amount of PG tracer bound to the well, which is inversely proportional to the amount of free PG present in the well during the incubation; or

$$\text{Absorbance} \propto [\text{Bound PG Tracer}] \propto 1/[\text{PG}]$$

4.3. In vivo anti-inflammatory activity

Male Wistar strain albino rats weighing 180–200 g were used throughout the assay. They were acquired from a closed randombred colony at the College of Agricultural and Veterinary Medicine, Al Qassim University, Kingdom of Saudi Arabia. Rats were given *ad libitum* access to food and water and housed in groups of four in isolated cages under standard conditions of light and temperature. The animals were acclimatized for 2 weeks prior to experiments. The investigation conformed to the guide for the Care and Use of Laboratory Animals published by US National Institute of Health (NIH Publication No.83–23, revised 1996). The Local Ethics Committee approved this study.

4.3.1. The carrageenan-induced rat paw edema model (acute inflammatory model)

The methods of Winter et al. [34] and Adeyemi et al. [35] were adopted. A total of seventeen groups of rats having 5 animals each were used for the study. In the control group, only the vehicle, 2% DMSO, was administered. Positive control groups were treated with diclofenac sodium or celecoxib. All drugs and compounds were given orally at the dose of 10 mg/kg. After 1 h, the rats were challenged with subcutaneous injection of 0.1 mL of freshly prepared solution of 1% of carrageenan (Sigma Aldrich, St. Louis, MO, USA) in sterile 0.9% normal saline was injected into the sub plantar region of the left hind paw under light ether anesthesia. An equal volume of saline was injected into the right hind paw and served as internal control for the degree of inflammation in the left hind paw. The paw edema was measured Plethysmographically (UgoBasile 7150, Varese, Italy Plethysmograph) and re-measured again 1, 2 and 4 h after injection of carrageenan. Edema was expressed as an increase in the volume of paw, and the percentage of edema inhibition (or percent protection against inflammation) for each rat and each group was calculated according to the following equation:

$$\%\ \text{Inhibition} = \frac{(\text{Vt} - \text{Vo})\ \text{control} - (\text{Vt} - \text{Vo})\ \text{test compound} \times 100}{(\text{Vt} - \text{Vo})\ \text{control}}$$

where Vt is the mean volume of edema at specific time interval and Vo is the mean volume of edema at zero time intervals.

4.3.2. Determination of effective dose 50 (ED_{50})

The selected compounds were further tested at 5, 10, 20, 40, and 50 mg/kg body weight and the ED_{50} was determined by measuring the inhibition of edema volume 3 h after carrageenan injection.

4.3.3. The carrageenan-induced rat paw edema model (sub-acute inflammatory model)

Rats in the first experiment were given the same test compounds daily for 7 successive days. A solution of carrageenan (1%, 0.1 mL) was injected into the sub planter region of the left hind paw under light ether anesthesia 1 h after oral administration of the test material. A second injection of carrageenan (1%, 0.1 mL) was given on the third day. The changes in the volume of paw were measured Plethymographically at the first and eighth days [34,35].

4.3.4. Turpentine oil–induced granuloma pouch bioassay

This chronic inflammatory model was performed as previously described [36] and modified using turpentine oil as irritant [37]. In ether-anaesthetized rats subcutaneously dorsal granuloma pouch was made by injecting 2 mL of air, followed by injecting 0.5 mL of turpentine oil into it. As mentioned previously, drugs and compounds were given orally at the dose of 10 mg/kg, one hour before turpentine oil injection and continued for seven consecutive days. On the eighth day, the pouch was opened under light ether anesthesia and the exudates were collected by a syringe. The volume (mL) of the exudates was measured and the percentage inhibition of inflammation relative to the control was determined as follows:

$$\%\ \text{Inhibition} = \frac{(\text{V control} - \text{V treated}) \times 100}{\text{V control}}$$

4.4. Computational methods

4.4.1. Proteins and ligands preparation

Crystal structures for COX-I and COX-II were downloaded from the protein data bank (PDB, ID: 3N8Z [38] and 3LN1 [39]) both of which were solved by X-ray diffraction (XRD). Then the co-crystallized ligand and all water molecules were removed from the protein structure. The protein structure was prepared by MOE using the protein preparation wizard [40]. This wizard prepares the crystal structure by checking the protein for any missing atoms, residues or loop; consequently, it performs all the required corrections. The structure was then processed by the Maestro protein preparation module to set up partial charges on each atom and protonation states on each ionizable group [41]. The co-crystallized ligand from the crystal structures was used to define the binding site of the COX enzymes then a grid box was created using the Receptor Grid Generation module in Glide [42]. The ten synthesized compounds were built using the build panel in MOE then were energy minimized via the Maestro program [42] and the OPLS force field [43].

4.4.2. Glide docking

Next, ligands were docked into the previously identified binding site using the Glide docking tool [42], where the extra-precision (XP) Algorithm [44] was used for conformational sampling. Next, the resulting poses were given scores via the Glide-XP scoring function which includes terms for van der Waals, hydrogen bond, electrostatic interactions, desolvation penalty and intra-ligand contact penalty [44].

Conflict of interest

The authors report no conflicts of interest. The authors alone are responsible for the contents and writing the paper.

Appendix A. Supplementary material

Supplementary data to this article can be found online at https://doi.org/10.1016/j.bioorg.2019.02.014.

References

[1] M. Bakavoli, G. Bagherzadeh, M. Vaseghifar, A. Shiri, M. Pordel, M. Mashreghi, P. Pordeli, M. Araghi, Eur. J. Med. Chem. 45 (2010) 647–650.
[2] K.J. Curran, J.C. Verheijen, J. Kaplan, D.J. Richard, L. Toral-Barza, I. Hollander, J. Lucas, S. Ayral-Kaloustian, K. Yu, A. Zask, Bioorg. Med. Chem. Lett. 20 (2010) 1440–1444.
[3] I. Kim, J.H. Song, C.M. Park, J.W. Jeong, H.R. Kim, J.R. Ha, Z. No, Y.L. Hyun, Y.S. Cho, N. Sook Kang, D.J. Jeon, Bioorg. Med. Chem. Lett. 20 (2010) 922–926.
[4] L. Yuan, C. Song, C. Li, Y. Li, L. Dong, S. Yin, Eur. J. Med. Chem. 67 (2013) 152–157.
[5] S. Schenone, C. Brullo, O. Bruno, F. Bondavalli, L. Mosti, G. Maga, E. Crespan, F. Carraro, F. Manetti, C. Tintori, M. Botta, Eur. J. Med. Chem. 43 (2008) 2665–2676.
[6] T. Wang, M.L. Lamb, D.A. Scott, H. Wang, M.H. Block, P.D. Lyne, J.W. Lee, A.M. Davies, H.J. Zhang, Y. Zhu, F. Gu, Y. Han, B. Wang, P.J. Mohr, R.J. Kaus, J.A. Josey, E. Hoffmann, K. Thress, T. Macintyre, H. Wang, C.A. Omer, D. Yu, J. Med. Chem. 51 (2008) 4672–4684.
[7] H. Mukaiyama, T. Nishimura, S. Kobayashi, Y. Komatsu, S. Kikuchi, T. Ozawa, N. Kamada, H. Ohnota, Bioorg. Med. Chem. 16 (2008) 909–921.
[8] P. Zang, M. Pennel, J. Wright, W. Chen, M. Leleti, Y. Li, L. Li, Y. Xu, PCT. Int. Appl. WO 2007002293, Chemocentryx, USA.
[9] S. Saggar, T. Tucker, R. Tynebor, D. Su, N. Anthony, US. Patent. Appl. US 20070214422007.
[10] J.D. Anderson, H.B. Cottam, S.B. Larson, L.D. Nord, G.R. Revankar, R.K. Robins, J. Heterocycl. Chem. 27 (1990) 439–453.
[11] J.L. Avila, M.A. Polegre, R.K. Robins, Comp. Biochem. Physiol. C: Pharmacol. Toxicol. Endrocrinol. 83 (1986) 291–294.
[12] J. Li, F. Zhao Yan, L. Zhao Xiang, Y. Yuan Xiao, P. Gong, Arch. Pharm. Chem. Life Sci. 339 (2006) 593–597.
[13] F. Manetti, A. Santucci, G.A. Locatelli, G. Maga, A. Spreafico, T. Serchi, M. Orlandini, G. Bernardini, N.P. Caradonna, A. Spallarossa, C. Brullo, S. Schenone, O. Bruno, A. Ranise, F. Bondavalli, O. Hoffmann, M. Bologna, A. Angelucci, M. Botta, J. Med. Chem. 50 (2007) 5579–5588.
[14] A. Feurer, J. Luithle, S. Wirtz, G. Koenig, J. Stasch, E. Stahl, R. Schreiber, F. Wunder, D. Lang, PCT. Int. Appl. WO 2004009589, Bayer Healthcare AG, Germany.
[15] X. Chen, J. Leng, K.P. Rakesh, N. Darshini, T. Shubhavathi, H.K. Vivek, N. Mallesha, H.-L. Qin, Med. Chem. Comm. 8 (2017) 1706–1719.
[16] C.S. Karthik, H.M. Manukumar, S. Sandeep, B.L. Sudarshan, S. Nagashree, L. Mallesha, K.P. Rakesh, K.R. Sanjay, P. Mallu, H.-L. Qin, Med. Chem. Comm. 9 (2018) 713–724.
[17] C. Li, M.B. Sridhara, K.P. Rakesh, H.K. Vivek, H.M. Manukumar, C.S. Shantharam, H.-L. Qin, Bioorg. Chem. 81 (2018) 389–395.
[18] H.M. Revankar, S.N.A. Bukhari, G.B. Kumar, H.-L. Qin, Bioorg. Chem. 71 (2017) 146–159.
[19] S.-M. Wang, G.-F. Zha, K.P. Rakesh, N. Darshini, T. Shubhavathi, H.K. Vivek, N. Mallesha, H.-L. Qin, Med. Chem. Comm. 8 (2017) 1173–1189.
[20] C. Zhao, K.P. Rakesh, L. Ravidar, W.-Y. Fang, H.-L. Qin, Eur. J. Med. Chem. 162 (2019) 679–734.
[21] L. Revesz, E. Blum, F.E. Di Padova, T. Buhl, R. Feifel, H. Gram, P. Hiestand, U. Manning, U. Neumann, G. Rucklin, Bioorg. Med. Chem. Lett. 16 (2006) 262–266.
[22] J. Das, R.V. Moquin, S. Pitt, R. Zhang, D.R. Shen, K.W. McIntyre, K. Gillooly, A.M. Doweyko, J.S. Sack, H. Zhang, S.E. Kiefer, K. Kish, M. McKinnon, J.C. Barrish, J.H. Dodd, G.L. Schieven, K. Leftheris, Bioorg. Med. Chem. Lett. 18 (2008) 2652–2657.
[23] C. Liu, J. Lin, S. Pitt, R.F. Zhang, J.S. Sack, S.E. Kiefer, K. Kish, A.M. Doweyko, H. Zhang, P.H. Marathe, J. Trzaskos, M. McKinnon, J.H. Dodd, J.C. Barrish, G.L. Schieven, K. Leftheris, Bioorg. Med. Chem. Lett. 18 (2008) 1874–1879.
[24] S.A. Rostom, I.M. el-Ashmawy, H.A. Abd el Razik, M.H. Badr, H.M. Ashour, Bioorg. Med. Chem. 17 (2009) 882–895.
[25] G. Dannhardt, W. Kiefer, Eur. J. Med. Chem. 36 (2001) 109–126.
[26] H. Yoshimura, S. Sekine, H. Adachi, Y. Uematsu, A. Mitani, N. Futaki, N. Shimizu, Protein Expr. Purif. 80 (2011) 41–46.
[27] K.G. Peri, P. Hardy, D.Y. Li, D.R. Varma, S. Chemtob, J. Biol. Chem. 270 (1995) 24615–24620.
[28] G. Menozzi, L. Merello, P. Fossa, L. Mosti, A. Piana, F. Mattioli, Farmaco 58 (2003) 795–808.
[29] A. Palomer, F. Cabre, J. Pascual, J. Campos, M.A. Trujillo, A. Entrena, M.A. Gallo, L. Garcia, D. Mauleon, A. Espinosa, J. Med. Chem. 45 (2002) 1402–1411.
[30] A.K. Tewari, P. Srivastava, V.P. Singh, A. Singh, R.K. Goel, C.G. Mohan, Chem. Pharm. Bull (Tokyo) 58 (2010) 634–638.
[31] A.M. Youssef, E.G. Neeland, E.B. Villanueva, M.S. White, I.M. El-Ashmawy, B. Patrick, A. Klegeris, A.S. Abd-El-Aziz, Bioorg. Med. Chem. 18 (2010) 5685–5696.
[32] C.C. Cheng, R.K. Robins, J. Org. Chem. 21 (1956) 1240–1256.
[33] K.C. Duggan, M.J. Walters, J. Musee, J.M. Harp, J.R. Kiefer, J.A. Oates, L.J. Marnett, J. Biol. Chem. 285 (2010) 34950–34959.
[34] C.A. Winter, E.A. Risley, G.W. Nuss, Proc. Soc. Exp. Biol. Med. 111 (1962) 544–547.
[35] O.O. Adeyemi, S.O. Okpo, O.O. Ogunti, Fitoterapia 73 (2002) 375–380.
[36] A. Robert, J.E. Nezamis, Acta Endocrinol. 25 (1957) 105–107.
[37] V.M. Shastry, V.R. Patil, R.Y. Chaudhari, Int. J. Pharm. Pharm. Sci. 3 (2011) 241–244.
[38] R.S. Sidhu, J.Y. Lee, C. Yuan, W.L. Smith, Biochemistry 49 (2010) 7069–7079.
[39] J.L. Wang, D. Limburg, M.J. Graneto, J. Springer, J.R. Hamper, S. Liao, J.L. Pawlitz, R.G. Kurumbail, T. Maziasz, J.J. Talley, J.R. Kiefer, J. Carter, Bioorg. Med. Chem. Lett. 20 (2010) 7159–7163.
[40] C.C. Group, Molecular Operating Environment.
[41] M. Brisson, T. Nguyen, A. Vogt, J. Yalowich, A. Giorgianni, D. Tobi, I. Bahar, C.R. Stephenson, P. Wipf, J.S. Lazo, Mol. Pharmacol. 66 (2004) 824–833.
[42] L. Schrödinger, Small-Molecule Drug Discovery Suite, in: Glide version 6.7, 2015.
[43] W.L. Jorgensen, J. Tirado-Rives, J. Am. Chem. Soc. 110 (1988) 1657–1666.
[44] R.A. Friesner, R.B. Murphy, M.P. Repasky, L.L. Frye, J.R. Greenwood, T.A. Halgren, P.C. Sanschagrin, D.T. Mainz, J. Med. Chem. 49 (2006) 6177–6196.